QUARTERLY JOURNAL OF THE ROYAL METEOROLOGICAL SOCIETY

How well do we understand the Planck feedback?

Timothy W. Cronin[1]*

[1]Program in Atmospheres, Ocean, and Climate, MIT, Cambridge, Massachusetts, USA

Correspondence
Timothy Cronin, Program in Atmospheres, Oceans, and Climate, MIT, 77 Massachusetts Ave., Cambridge, MA 02139, USA.
Email: twcronin@mit.edu

Funding information
NSF Atmospheric Chemistry grant AGS-1906719: "Advancing the Understanding of the Impacts of Wave-Induced Temperature Fluctuations on Atmospheric Chemistry."

The increase in planetary infrared energy loss with vertically uniform warming of the surface and troposphere, called the Planck feedback (λ_P) in climate models, provides a key starting point for feedback analysis of climate change; λ_P^{-1} defines a "no-feedback" climate sensitivity. Calculations from climate models give $\lambda_P \approx 3.3$ W m^{-2} K^{-1}, ~ 0.5 W m^{-2} K^{-1} smaller than a simple estimate $\overline{\lambda_e} = 4\sigma\overline{T_e}^3$ based on Earth's outgoing longwave radiation. This ~ 0.5 W m^{-2} K^{-1} discrepancy represents a large and unstudied gap in our understanding of Earth's "no-feedback" climate sensitivity. In this paper, I use radiative transfer physics and a line-by-line model to define and quantify four correction terms that cause the Planck feedback to deviate from $4\sigma\overline{T_e}^3$. Of the four terms, the stratospheric masking correction, which owes to the lack of stratospheric warming in calculation of the Planck feedback, plays the largest role, destabilizing λ_P by ~ 0.35 W m^{-2} K^{-1} relative to λ_e. I also find that both stratospheric masking and another smaller correction term, related to temperature-dependent absorption properties of greenhouse gases, cause λ_P to vary about 30% more with surface temperature than does λ_e. These results paint a more nuanced picture of a climate feedback widely considered to be trivial, and suggest that the stability of much different climates could deviate from our expectations.

KEYWORDS
Climate feedbacks, Climate change, Atmospheric radiation, Planetary atmospheres

1 | INTRODUCTION

The global Planck feedback, $\overline{\lambda_P}$, or rate of increase of infrared energy loss per unit vertically uniform warming of the surface and troposphere, is the dominant stabilizing feedback in planetary climate. An estimate of its magnitude is given by the derivative of the Stefan-Boltzmann law with respect to temperature, $\overline{\lambda_e} = 4\sigma\overline{T_e}^3$ – evaluated at a global effective emission temperature $\overline{T_e}$, which is defined so that $\sigma\overline{T_e}^4$ equals the planetary-average outgoing longwave radiation (OLR). Earth's average OLR of 240 W m^{-2} corresponds to an effective emission temperature of 255 K, and a consequent Planck feedback estimate of $\overline{\lambda_e} = 3.76$ W m^{-2} K^{-1}. Feedback analysis of comprehensive general circulation models (GCMs), however, gives a Planck feedback of 3.27 W m^{-2} K^{-1} – roughly 0.5 W m^{-2} K^{-1} more positive than $\overline{\lambda_e}$ (Zelinka et al., 2020; Soden and Held, 2006). This missing 0.5 W m^{-2} K^{-1} seems to vary little among climate models, but has not been studied carefully and represents a notable gap in our understanding of Earth's dominant stabilizing climate feedback. In this paper, I attempt to close this gap and account for the discrepancy between the global Planck feedback $\overline{\lambda_P}$ and the estimate $\overline{\lambda_e} = 4\sigma\overline{T_e}^3$.

Although the Planck feedback is a stabilizing or negative feedback, throughout this paper I will use a positive-definite sign convention for it, so that a "larger Planck feedback" is more stabilizing and a "smaller Planck feedback" is less stabilizing; corrections that are positive in sign are thus stabilizing and those that are negative are destabilizing. I define the global-mean Planck feedback as equal to the estimate $4\sigma\overline{T_e}^3$, plus a set of additive corrections that correspond to specific mechanisms. First, the global Planck feedback is a temperature-change weighted average of local Planck feedbacks, rather than a simple average, and regions with a smaller local Planck feedback (high latitudes) tend to warm more than regions with a larger Planck feedback (low latitudes). Since the planet warms more where the feedback is small, meridional covariance of local feedbacks and warming decreases the global Planck feedback. Second, the Planck feedback is calculated based on the increase in OLR from tropospheric and surface warming only, with no stratospheric temperature change, so increases in OLR are muted in spectral regions where the stratosphere is optically thick; I refer to this as the stratospheric masking correction and it strongly decreases the local Planck feedback. Third, the absorption coefficients of most gases vary with temperature. I denote changes in OLR with warming due solely to changes in optical properties of greenhouse gases as the temperature-dependent opacity correction; it also tends to decrease the local Planck feedback, primarily due to increasing opacity with warming on the flanks of the CO_2 ro-vibrational band. The fourth correction, nonlinear averaging, arises because the Planck feedback is given by the nonlinear derivative of the Planck function with respect to temperature, integrated over a range of both emitting temperatures and wavenumbers. The effects of nonlinear averaging over two variables – emitting temperatures and wavenumber – motivates further decomposition of Δ_N, into a multi-blackbody nonlinearity Δ_M and a spectral nonlinearity Δ_ν. A small negative contribution from Δ_M is offset by a larger positive contribution from Δ_ν, making the Planck feedback larger and closer to $\overline{\lambda_e} = 4\sigma\overline{T_e}^3$. To summarize, I consider four specific corrections:

$$
\begin{aligned}
\overline{\lambda_P} \quad &= \quad \overline{\lambda_e} + \Delta_C + \Delta_S + \Delta_T + \Delta_N \qquad (1)\\
\Delta_C \quad &: \quad \text{meridional covariance}\\
\Delta_S \quad &: \quad \text{stratospheric masking}\\
\Delta_T \quad &: \quad \text{temperature} - \text{dependent opacity}\\
\Delta_N \quad &: \quad \text{nonlinear averaging;}
\end{aligned}
$$

these are listed roughly in order of increasing complexity. The stratospheric masking correction appears to be the single most important term.

A possible reason why this 0.5 W m^{-2} K^{-1} discrepancy between $\overline{\lambda_P}$ and $\overline{\lambda_e}$ has gone unstudied is that the Planck feedback has been estimated previously as:

$$\overline{\lambda_e}' = 4\sigma\epsilon\overline{T_g}^3, \quad \text{(incorrect!)} \tag{2}$$

rather than $4\sigma\overline{T_e}^3$ (e.g., Cess et al., 1990; Feldl and Roe, 2013). Here $\overline{T_g}$ is the global-average surface temperature and ϵ is defined so that OLR= $\epsilon\sigma\overline{T_g}^4$. Using a global-mean surface temperature of $\overline{T_g} \approx 288$ K and OLR of 240 W m^{-2} implies $\epsilon \approx 0.6$, and thus that this feedback would be 3.3 W m^{-2} K^{-1} – close enough to $\overline{\lambda_P}$ that perhaps no discrepancy needs explaining. As suggested by the commentary in equation 2, however, the linear emissivity factor in this estimate is inconsistent with vertically uniform warming. Defining ϵ using OLR= $\epsilon\sigma\overline{T_g}^4$ implies that $\overline{T_e} = \epsilon^{1/4}\overline{T_g}$, and vertically uniform warming implies that the emission temperature warms by the same amount as the surface temperature, so the correct simple estimate of the of the Planck feedback should be:

$$\overline{\lambda_e} = 4\sigma\overline{T_e}^3 = 4\sigma\epsilon^{3/4}\overline{T_g}^3 \quad \text{(correct)}. \tag{3}$$

This is larger than $4\sigma\epsilon\overline{T_g}^3$ by a factor of $1/\epsilon^{1/4} \approx 1.14$. The extra factor of $\epsilon^{1/4}$ could be physically justified in equation 2 only if the warming at the emission level were smaller than that at the surface by a factor of $\epsilon^{1/4}$ – but this contradicts how the feedback is computed in comprehensive models (e.g., Soden et al., 2008). Only by coincidence does $\overline{\lambda_e}'$ lie close to detailed calculations of $\overline{\lambda_P}$, and it does not confer any real physical understanding of the 0.5 W m^{-2} K^{-1} gap described above.

A total deviation of 15% between $\overline{\lambda_P}$ and $\overline{\lambda_e}$ might seem minor, and decomposing such a deviation into several components might seem like an exercise in splitting hairs, particularly since climate models agree so closely on the value of the Planck feedback. The implications would be striking, however, if the Planck feedback were 0.5 W m^{-2} K^{-1} more stabilizing and all other feedbacks remained the same. Zelinka et al. (2020) show that the net climate feedback in climate models from the coupled model intercomparison project, phases 5 and 6 (CMIP5 and CMIP6) averages 1 W m^{-2} K^{-1}. Adding 0.5 W m^{-2} K^{-1} to this would reduce total climate sensitivity by a third, and dramatically reduce the intermodel spread in climate sensitivity as well. It seems imprudent to allow such a large unexplained gap in Earth's "no-feedback" climate sensitivity to persist without a thorough understanding of why it arises, and upon what aspects of the climate system it depends.

In this paper, I define and quantify the corrections needed to close the 0.5 W m^{-2} K^{-1} gap between $\overline{\lambda_P}$ and $\overline{\lambda_e}$. I begin by presenting background on each of the four mechanisms that alter the global Planck feedback (Section 2); this provides a full explanation of why meridional covariance can reduce the global Planck feedback. I then describe numerical calculations with a radiative transfer model that allow quantification of the other three mechanisms (Section 3), and describe my findings (Section 4). I conclude by discussing some of the limitations of this work and by speculating about situations where the gap between λ_P and λ_e could be appreciably larger (Section 5).

2 | MECHANISMS

2.1 | Meridional covariance

The meridional covariance correction, Δ_C, depends solely on the climatological pattern of warming and its covariance with the locally defined Planck feedback, so its sign and magnitude can be estimated by referring to previous work. Since Δ_C also turns out to be large in magnitude, it makes sense to define first.

The global-average Planck feedback, $\overline{\lambda_P}$, is a weighted average of local Planck feedbacks multiplied by local temperature changes. Considering the structure of feedbacks and temperature changes (T') in latitude only, with $x = \sin\phi$, gives:

$$\overline{\lambda_P} = \frac{\int_{-1}^{1} \lambda_P(x) T'(x) dx}{\int_{-1}^{1} T'(x) dx}. \tag{4}$$

The correction to the global-mean Planck feedback due to meridional covariance, Δ_C, is given by the difference between $\overline{\lambda_P}$ for a given warming pattern $T'(x)$, and that which would be obtained for globally uniform warming:

$$\Delta_C = \frac{\int_{-1}^{1} \lambda_P(x) T'(x) dx}{\int_{-1}^{1} T'(x) dx} - \int_{-1}^{1} \lambda_P(x) dx. \tag{5}$$

To proceed further, I assume that the meridional structure of $T'(x)$ and $\lambda_P(x)$ can be written as Legendre polynomials $P_n(x)$ and truncated at their second-order terms, so that $T'(x) \approx T_0' + T_2' P_2(x)$ and $\lambda_P(x) \approx \lambda_{P,0} + \lambda_{P,2} P_2(x)$. Here, $P_2(x) = (3x^2 - 1)/2$ is the second Legendre polynomial and describes well the structure of both the climatological meridional temperature distribution and the polar-amplified warming pattern seen in simple models (e.g., North and Coakley, 1979; Merlis and Henry, 2018). It follows from the orthogonality of Legendre polynomials under integration over $x \in [-1, 1]$ that:

$$\begin{aligned} \overline{\lambda_P} &\approx \lambda_{P,0} + \frac{2\lambda_{P,2} T_2'}{5 T_0'} \\ \Delta_C &\approx \frac{2\lambda_{P,2} T_2'}{5 T_0'}. \end{aligned} \tag{6}$$

Furthermore, if the meridional structure of warming is similar regardless of magnitude, so that $T_2' \approx a T_0'$, and writing $\lambda_{P,2} = b\lambda_{P,0}$, a particularly simple form emerges: $\Delta_C \approx (2ab/5)\lambda_{P,0}$. Global models show strong polar amplification, so $a > 0$, and the local Planck feedback is smaller at high latitudes than low latitudes, so $b < 0$. Polar warming twice that of the global mean corresponds to $a \approx 1$, and polar Planck feedbacks that are about 1 W m^{-2} K^{-1} smaller than tropical values (e.g., 2.5 W m^{-2} K^{-1} as compared to 3.5 W m^{-2} K^{-1}, Soden et al., 2008) corresponds to $b \approx -1/5$. Together these estimates give a back-of-the envelope value of $\Delta_C \approx -0.08\lambda_{P,0} \approx -0.25$ W m^{-2} K^{-1}. Thus, meridional covariance is likely a large correction, explaining perhaps as much as half the deviation between $\overline{\lambda_e}$ and $\overline{\lambda_P}$.

A more exact calculation of Δ_C could be made based on the exact spatiotemporal structure of warming in a given model together with radiative kernel or partial radiative perturbation calculations. Such calculations are deferred to future work, however, and I now turn to the remaining corrections that contribute to the local deviation of λ_P from λ_e, which require an explanation in terms of the physics of radiative transfer.

2.2 | The local correction terms

I first define terminology and notation that will be used throughout the paper. To avoid confusion between Greek letters, the electromagnetic spectrum throughout this paper is referred to by the wavenumber, $\tilde{\nu}$, equal to the reciprocal of the wavelength, and expressed conventionally in units of cm^{-1}. For a given temperature profile, the monochromatic flux at the top of the atmosphere, $F_0^{\tilde{\nu}}$ (units W m^{-2} cm), is given by:

$$F_0^{\tilde{\nu}} = \pi B^{\tilde{\nu}}(T_g) e^{-\tau_0} + \int_0^{\tau_0} \pi B^{\tilde{\nu}}(T(\tau')) e^{-\tau'} d\tau'. \tag{7}$$

Here, τ_0 is the total optical thickness of the atmosphere at wavenumber $\tilde{\nu}$ and accounts for integration along a representative slant path for upward irradiance, the integration is over optical thickness from $\tau = 0$ at the top of the atmosphere to τ_0 at the surface, and T_g is the surface temperature. Monochromatic fluxes are indicated with a superscript $^{\tilde{\nu}}$ and spectrally integrated fluxes without a superscript; it should also be understood that optical thickness τ and emissivity ϵ depend on wavenumber wherever used, as they lack meaningful direct integrals over wavenumber. I also indicate the level where fluxes are defined with a subscript: $_0$ for the top of the atmopshere and $_T$ for the tropopause. The Planck function, $B^{\tilde{\nu}}(T)$, describes the radiance of a blackbody at temperature T:

$$B^{\tilde{\nu}}(T) = \frac{2\pi hc^2\tilde{\nu}^3}{\exp\left(\frac{hc\tilde{\nu}}{kT}\right) - 1}, \tag{8}$$

where h is Planck's constant, c is the speed of light, and k is Boltzmann's constant. The integral of the Planck function over all wavenumbers defines the Stefan-Boltzmann law $\pi B(T) = \int_0^\infty \pi B^{\tilde{\nu}}(T) d\tilde{\nu} = \sigma T^4$. When writing the temperature derivative of the Planck function, $dB^{\tilde{\nu}}(T_x)/dT$, I use the argument of the Planck function (here, T_x) to indicate the temperature at which the derivative is evaluated.

Since both the monochromatic and spectrally integrated Planck functions increase monotonically with temperature, a given spectrally integrated flux F (units W m^{-2}) or monochromatic flux $F^{\tilde{\nu}}$ can be characterized by the temperature of an equivalent radiating blackbody:

$$T_e = \left(\frac{F}{\sigma}\right)^{1/4} \tag{9}$$

$$T_b^{\tilde{\nu}} = \frac{hc\tilde{\nu}}{k} \ln^{-1}\left[1 + \frac{2\pi hc^2\tilde{\nu}^3}{F^{\tilde{\nu}}}\right]. \tag{10}$$

I refer to T_e as the effective emission temperature, and $T_b^{\tilde{\nu}}$ as the monochromatic brightness temperature.

In general, equation 7 suggests that if the atmosphere and surface are warmed at all heights, $F_0^{\tilde{\nu}}$ will increase because $dB^{\tilde{\nu}}/dT > 0$. However, there are additional contributions to the change in flux $dF_0^{\tilde{\nu}}/dT$ because the optical thickness of gases also depends on temperature. The total change in flux ($dF_0^{\tilde{\nu}}/dT$) from a warming atmosphere and surface can be written as a sum of contributions from an increasing Planck function source $(dF_0^{\tilde{\nu}}/dT)_{\text{Planck}}$ and from temperature-dependent optical thickness $(dF_0^{\tilde{\nu}}/dT)_{\text{optics}}$. The contribution from increasing thermal emission alone is:

$$\left(\frac{dF_0^{\tilde{\nu}}}{dT}\right)_{\text{Planck}} = \pi \frac{dB^{\tilde{\nu}}(T_g)}{dT} e^{-\tau_0} + \int_0^{\tau_0} \pi \frac{dB^{\tilde{\nu}}(T(\tau'))}{dT} e^{-\tau'} d\tau'. \tag{11}$$

Although $(dF_0^{\tilde{\nu}}/dT)_{\text{optics}}$ is harder to write out explicitly, it can be isolated using radiative transfer calculations where the temperature seen by the Planck function source is held constant, but calculations of gas optics see a temperature increased by 1K.

The Planck feedback in GCMs is calculated as the change in top-of-atmosphere flux from warming only the troposphere and surface:

$$\lambda_P = \int_0^\infty \left[\left(\frac{dF_0^{\tilde{\nu}}}{dT_T} \right)_{\text{Planck}} + \left(\frac{dF_0^{\tilde{\nu}}}{dT_T} \right)_{\text{optics}} \right] d\tilde{\nu}, \tag{12}$$

where the derivative with respect to T_T indicates a vertically uniform surface and tropospheric warming. This is often computed by summing the tropospheric and surface temperature kernel, which will include effects from both increasing thermal emission and changing optical thickness.

With these definitions, the Planck feedback λ_P and estimated OLR-based feedback $\lambda_e = 4\sigma T_e^3 = \int_0^\infty \pi \left(dB^{\tilde{\nu}}(T_e)/dT \right) d\tilde{\nu}$ can finally be compared directly:

$$\lambda_P = \lambda_e + \underbrace{\int_0^\infty \left[\left(\frac{dF_0^{\tilde{\nu}}}{dT_T} \right)_{\text{Planck}} + \left(\frac{dF_0^{\tilde{\nu}}}{dT_S} \right)_{\text{Planck}} - \pi \frac{dB^{\tilde{\nu}}(T_e)}{dT} \right] d\tilde{\nu}}_{\Delta_N} + \underbrace{\int_0^\infty \left(\frac{dF_0^{\tilde{\nu}}}{dT_T} \right)_{\text{optics}} d\tilde{\nu}}_{\Delta_T} - \underbrace{\int_0^\infty \left(\frac{dF_0^{\tilde{\nu}}}{dT_S} \right)_{\text{Planck}} d\tilde{\nu}}_{\Delta_S}, \tag{13}$$

where each underbrace defines a correction term with physical meaning corresponding to that in Equation 1, and derivatives with respect to T_S indicate vertically uniform stratospheric warming. Equation 13 is a key result of this paper, and is an equality by construction, in that there should be no further residuals. I briefly discuss each correction term below, including a further decomposition of Δ_N into two parts.

2.2.1 | Stratospheric masking

In spectral regions where the stratosphere is optically thick, the flux at the top of the atmosphere will change little or not at all in response to warming of only the surface and troposphere, since the stratosphere masks the increase in upward flux at the tropopause. Thus, the monochromatic Planck feedback in these spectral regions may be close to zero. Assuming for illustrative purposes an isothermal stratosphere at temperature T_S, the upward monochromatic flux at the top-of-atmosphere, $F_0^{\tilde{\nu}}$, is given by:

$$F_0^{\tilde{\nu}} = (1 - \epsilon_S) F_T^{\tilde{\nu}} - \epsilon_S \pi B^{\tilde{\nu}}(T_S), \tag{14}$$

where $F_T^{\tilde{\nu}}$ is the upwelling monochromatic flux at the tropopause, and $\epsilon_S = (1 - e^{-\tau_S})$ defines the stratospheric emissivity in terms of stratospheric optical thickness at wavenumber $\tilde{\nu}$. Applying equation 13 for an isothermal stratosphere, the stratospheric masking correction simplifies to:

$$\Delta_S^{\tilde{\nu}} = -\left(\frac{dF_0^{\tilde{\nu}}}{dT_S} \right)_{\text{Planck}} = -\epsilon_S \pi \frac{dB^{\tilde{\nu}}(T_S)}{dT}. \tag{15}$$

The stratospheric masking correction must be negative, and will be largest in spectral regions where the stratospheric emissivity is close to 1 (or where $\tau_S >> 1$). Note that the assumption of an isothermal stratosphere here has been made for simplicity and analytic tractability; vertical temperature variations in the stratosphere would require an integral (over height) of $dB^{\tilde{\nu}}/dT$ multiplied by the differential transmissivity at each wavenumber in order to calculate $\Delta_S^{\tilde{\nu}}$.

2.2.2 | Temperature-dependent opacity

Although the dominant effect of warming at constant atmospheric composition is to increase the Planck function source, the optical properties of most greenhouse gases also depend on temperature. Equation 13 defines the correction $\Delta_T^{\tilde{\nu}}$ as the change in outgoing flux solely due to the alteration of tropospheric optical properties with warming, without any change in the Planck function source of thermal emission:

$$\Delta_T^{\tilde{\nu}} = \left(\frac{dF_0^{\tilde{\nu}}}{dT_T}\right)_{\text{optics}} = (1 - \epsilon_S)\left(\frac{dF_T^{\tilde{\nu}}}{dT_T}\right)_{\text{optics}}. \tag{16}$$

Temperature-dependence of atmospheric optical thickness occurs because absorption of photons by a gas depends not only on the abundance of that gas, but also on the population of molecules in the lower-level state of a quantum transition that allows for absorption of a photon of wavenumber $\tilde{\nu}$. In local thermodynamic equilibrium, this population is mediated by temperature, and higher energies of the lower-level state lead to larger relative increases in population with warming (expressions for the temperature-dependence of line strength are given in Appendix A). Especially for lines that are weak because lower-level molecular populations are small, an increase in temperature can cause a large relative increase in line strength. Strong lines and continuum regions, on the other hand, tend to absorb less with warming. For strong lines, weaker absorption is driven by the excitation of molecules out of the lower-level quantum state that can undergo the strong-line transition. For continuum regions, the physical underpinning for decreasing absorption with temperature is still under debate, but the empirical evidence for it is nonetheless clear (e.g., Cormier et al., 2005; Shine et al., 2012). Lest the reader find these temperature-dependencies of gas optics insufficiently complex, line widths also decrease slightly with warming, because collisional broadening depends on collisional frequency, which at constant pressure scales with the product of molecular speeds ($\propto T^{1/2}$) and density ($\propto T^{-1}$). Overall, temperature-dependent opacity can be summarized by the idea that some greenhouse gases become more effective with warming, while others may become less effective with warming.

2.2.3 | Nonlinear averaging

The Planck function (equation 8) is nonlinear in temperature, with the degree of nonlinearity becoming greater for higher wavenumbers. Furthermore, emission to space occurs from a range of temperatures – both at a given wavenumber and when considered across the spectrum. Thus, the increase in flux with warming will differ from the derivative of the flux of a blackbody with respect to temperature (evaluated at T_e or $T_b^{\tilde{\nu}}$). I divide this nonlinear-averaging correction:

$$\Delta_N = \int_0^\infty \left[\left(\frac{dF_0^{\tilde{\nu}}}{dT_T}\right)_{\text{Planck}} + \left(\frac{dF_0^{\tilde{\nu}}}{dT_S}\right)_{\text{Planck}} - \pi\frac{dB^{\tilde{\nu}}(T_e)}{dT}\right] d\tilde{\nu} \tag{17}$$

into two components – multiple-blackbody nonlinearity Δ_M and spectral nonlinearity Δ_ν.

Multiple-blackbody nonlinearity occurs for a collection of blackbodies at different temperatures, each of which contributes partially to the outgoing flux at the top of the atmosphere, because $B^{\tilde{\nu}}(T)$ and $dB^{\tilde{\nu}}(T)/dT$ are different nonlinear functions of temperature. The estimated flux increase $dB^{\tilde{\nu}}(T_b^{\tilde{\nu}})/dT$, evaluated at a brightness temperature $T_b^{\tilde{\nu}}$ representative of the average top-of-atmosphere flux $F_0^{\tilde{\nu}} = \sum w_i B^{\tilde{\nu}}(T_i)$ from a collection of blackbodies with temperatures T_i and weights w_i (where $\sum w_i = 1$), will generally differ from the flux increase for a vertically uniform warming, which equals $\sum w_i dB^{\tilde{\nu}}(T_i)/dT$. Here, a "collection of blackbodies" can refer to either a surface of heterogeneous temperature with no overlying absorbers, or to emission from different heights and temperatures within a single column of the atmosphere. The correction for multi-blackbody nonlinearity at each wavenumber, $\Delta_M^{\tilde{\nu}}$, can be written as the difference between the increased thermal emission caused by uniform warming of the surface, troposphere, and stratosphere $\left(dF_0^{\tilde{\nu}}/dT_T\right)_{\text{Planck}} + \left(dF_0^{\tilde{\nu}}/dT_S\right)_{\text{Planck}}$ and the derivative of the blackbody flux at the monochromatic brightness temperature $T_b^{\tilde{\nu}}$:

$$\Delta_M^{\tilde{\nu}} = \left(\frac{dF_0^{\tilde{\nu}}}{dT_T}\right)_{\text{Planck}} + \left(\frac{dF_0^{\tilde{\nu}}}{dT_S}\right)_{\text{Planck}} - \pi\frac{dB^{\tilde{\nu}}(T_b^{\tilde{\nu}})}{dT}. \tag{18}$$

The sign of this correction is not obvious, but Appendix B shows that the multi-blackbody nonlinearity for spectrally integrated fluxes must be less than or equal to 0; that is, $4\sigma\left[\sum_{i=1}^n w_i T_i^3\right] \leq 4\sigma\left[\sum_{i=1}^n w_i T_i^4\right]^{3/4} = 4\sigma T_e^3$. Extending this reasoning to monochromatic fluxes suggests $\Delta_M^{\tilde{\nu}}$ will generally be negative, and that the magnitude of $\Delta_M^{\tilde{\nu}}$ will scale with the variance of temperatures that emit to space at a given wavenumber.

Spectral nonlinearity occurs because the brightness temperature varies with wavenumber, and because the derivative of the Planck function, $dB^{\tilde{\nu}}(T)/dT$, is maximized at higher wavenumbers than the Planck function itself. For a blackbody, if the spectrum is split into high-wavenumber and low-wavenumber halves with equal total flux by a cutoff $\tilde{\nu}_m \approx 3.5kT/(hc)$, then roughly 2/3 of the increase in flux with warming comes from higher wavenumbers with $\tilde{\nu} > \tilde{\nu}_m$. I define the spectral nonlinearity correction as:

$$\Delta_\nu^{\tilde{\nu}} = \pi\frac{dB^{\tilde{\nu}}(T_b^{\tilde{\nu}})}{dT} - \pi\frac{dB^{\tilde{\nu}}(T_e)}{dT}; \tag{19}$$

which gives $\Delta_\nu = \int_0^\infty \pi(dB^{\tilde{\nu}}(T_b^{\tilde{\nu}})/dT)d\tilde{\nu} - \pi dB(T_e)/dT$ when integrated over wavenumber. The spectral nonlinearity correction is related to the covariance between $T_b^{\tilde{\nu}}$ and $dB^{\tilde{\nu}}(T)/dT$, which may in general be either positive or negative. For Earth, the presence of the water vapor spectral window where $T_b^{\tilde{\nu}}$ is high at wavenumbers near the peak in $dB^{\tilde{\nu}}(T)/dT$, together with the strong water vapor rotational band absorption where $T_b^{\tilde{\nu}}$ is low at wavenumbers with small $dB^{\tilde{\nu}}(T)/dT$, tend to make this covariance positive. This means that Δ_ν is usually positive, increasing the Planck feedback relative to λ_e.

3 | METHODS

I use calculations with the line-by-line radiative transfer model LBLRTM (Clough et al., 2005) to quantify the locally defined Planck feedback (local OLR change per unit local warming, e.g., Feldl and Roe, 2013), as well as the correction terms Δ_S, Δ_T, and $\Delta_N = \Delta_M + \Delta_\nu$. I use a spectral resolution of $\delta\tilde{\nu} \sim 0.01$ cm^{-1} over the thermal infrared from $\tilde{\nu} = 10 - 3500$ cm^{-1}, so a few hundred thousand monochromatic radiative transfer calculations are done for each profile. This allows for the effects of individual lines (typically with widths ~0.1 cm^{-1} at sea-level pressure) to be resolved. Output is interpolated to a 0.01 cm^{-1} grid and also averaged over 5 cm^{-1} intervals for purposes of plotting.

I create a set of reference atmospheric profiles by varying the whole temperature and moisture profile along with the surface temperature T_g. The surface pressure is set to 1000 hPa, and the 1000-hPa air temperature equals the surface temperature. Above this, temperatures decrease with height following the saturated pseudoadiabatic lapse rate, until reaching an isothermal stratosphere, taken to have a temperature $T_S = 200$ K. The vertical grid spacing is 500 m and fluxes are integrated to a height of 50 km. The troposphere is defined as all levels with $T > T_S$, and has relative humidity of 80% at all heights. The specific humidity in the stratosphere is set to a constant of 5×10^{-3} g kg^{-1}, and the ozone profile follows the gamma distribution in pressure from Wing et al. (2018):

$$r_{O_3} = 3.6478 \times 10^{-6} p^{0.83209} e^{-p/11.3515}, \tag{20}$$

where r_{O_3} is the ozone volume mixing ratio, and p is the atmospheric pressure in hPa. Unless otherwise specified, reference atmospheric profiles include 400 ppmv of CO_2, and no other well-mixed greenhouse gases. The dry atmosphere is taken to be 79% N_2 and 21% O_2 (relevant for pressure-broadening of lines). Gas absorber amounts are scaled by a factor of 5/3 to account for the slant path taken by thermal radiation through the atmosphere.

For each atmospheric profile, I run several calculations to determine the feedbacks λ_P and λ_e, and estimate the corrections Δ_S, Δ_T, and $\Delta_N = \Delta_M + \Delta_\nu$:

1. A control calculation gives a reference infrared flux spectrum $F_0^{\tilde{\nu}}$ and thus defines $T_e = (\int_0^\infty F_0^{\tilde{\nu}} d\tilde{\nu}/\sigma)^{1/4}$ and $\lambda_e = 4\sigma T_e^3$.
2. A troposphere-warmed calculation uses tropospheric and surface temperatures 1 K warmer than the control calculation. The flux difference between this calculation and the control approximates $dF_0^{\tilde{\nu}}/dT_T$ and thus gives:

$$\lambda_P = \int_0^\infty (dF_0^{\tilde{\nu}}/dT_T) d\tilde{\nu}. \tag{21}$$

3. A tropopause-flux control calculation defines $F_T^{\tilde{\nu}}$.
4. A tropopause-flux troposphere-warmed calculation gives an estimate of $dF_T^{\tilde{\nu}}/dT_T$, from which I calculate the stratospheric emissivity (and thus Δ_S following equation 15) as:

$$\epsilon_S = 1 - \frac{dF_0^{\tilde{\nu}}/dT_T}{dF_T^{\tilde{\nu}}/dT_T}. \tag{22}$$

5. A tropopause-flux gas-optics-only warmed calculation adjusts optical properties of greenhouse gases in the troposphere to correspond to a temperature warmed by 1 K relative to the control, but the Planck function source is unperturbed. The flux difference between this calculation and the tropopause-flux control gives a direct estimate of $\left(dF_T^{\tilde{\nu}}/dT_T\right)_{\text{optics}}$ and thus of $\Delta_T^{\tilde{\nu}}$ after multiplying by $(1-\epsilon_S)$ to account for stratospheric attenuation (following equation 16).

The monochromatic brightness temperatures $T_b^{\tilde{\nu}}$ from the control simulation then enable calculation of the correction terms Δ_M and Δ_ν, following equations 18 and 19.

4 | RESULTS

I first describe the calculated spectrum of OLR, feedbacks, and corrections, for a reference-state atmosphere with $T_S = 290$ K (close to the global-mean surface temperature). The OLR shows absorption lines across the entire spectrum, but most strongly from a carbon dioxide ro-vibrational complex between 550 and 750 cm^{-1}, from an ozone ro-vibrational complex near 1050 cm^{-1}, from the pure rotational band of water vapor at 0-500 cm^{-1} and a ro-vibrational water vapor feature from 1250-2000 cm^{-1} (Figure 1a). This reference atmosphere has OLR=249.4 W m^{-2}, an effective emission temperature $T_e = 257.5$ K, and thus an estimated local feedback of $\lambda_e = 4\sigma T_e^3 = 3.87$ W m^{-2} K^{-1}.

A calculation with the surface and troposphere warmed by 1K, however, shows that the Planck feedback is only

$\lambda_P = 3.52$ W m^{-2} K^{-1}, 0.35 W m^{-2} K^{-1} less than λ_e (Figure 1b). The difference is explained completely by $\Delta_S = -0.35$ W m^{-2} K^{-1} (spectrum $\Delta_S^{\tilde{\nu}}$ shown as blue line in Figure 1b), with negative corrections from temperature-dependent opacity and multi-blackbody nonlinearity $\Delta_T = -0.09$ W m^{-2} K^{-1} and $\Delta_M = -0.02$ W m^{-2} K^{-1} almost exactly offsetting the positive correction from spectral nonlinearity $\Delta_\nu = +0.11$ W m^{-2} K^{-1} (Figure 1b). I elaborate on the spectral characteristics of each correction below, then describe how each correction depends on atmospheric temperature.

4.1 | Stratospheric masking

The pink and red lines in Figure 1b show several regions of nearly zero increase with warming, most strikingly in the center of the CO_2 ro-vibrational band. These regions where $dF_0^{\tilde{\nu}}/dT_T$ dips well below $dB^{\tilde{\nu}}(T_S)/dT$ indicate wavenumbers where the stratosphere is optically thick; since the stratosphere is not warmed, these spectral regions show little or no change in outgoing flux. The negative-definite correction term $\Delta_S^{\tilde{\nu}}$ has largest magnitudes in the CO_2 ro-vibrational band, the Ozone ro-vibrational band (near 1000 cm^{-1}), and the strongest parts of the H_2O rotational band – the parts of the spectrum where the stratosphere is optically thickest in the infrared. The cumulative integral of Δ_S as a function of wavenumber, $\int_0^{\tilde{\nu}} \Delta_S^{\tilde{\nu}'} d\tilde{\nu}'$ indicates that ~60% of the stratospheric masking correction comes from CO_2, ~25% from H_2O, and ~15% from O_3 (Figure 2).

4.2 | Temperature-dependent opacity

Increasing the temperature in LBLRTM seen by the gas-optics calculations but not by the Planck function source gives an estimate of the temperature-dependent opacity correction, $\Delta_T^{\tilde{\nu}}$ (gold line in Figure 1b). This correction is most negative on the flanks of the CO_2 ro-vibrational feature, on the high-wavenumber edge of the H_2O rotational band, and on the low-wavenumber edge of the H_2O ro-vibrational band, most positive in the water vapor continuum absorption region from 800-1000 cm^{-1}, and small elsewhere. Line strengths at the edges of ro-vibrational and rotational features depend particularly strongly on temperature because their lower-level states have high rotational quantum numbers and thus high lower-level energies ($\tilde{\nu}_l$). Furthermore, these regions tend not to be too optically thick, so most of the flux difference at the tropopause is transmitted through the stratosphere (the factor $(1-\epsilon_S)$ in Equation 16). Stratospheric optical thickness makes $\Delta_T^{\tilde{\nu}}$ small in the core of the CO_2, H_2O, and O_3 absorption features, where the stratospheric masking correction is most negative. The cumulative integral of Δ_T in wavenumber shows that about half of it comes from CO_2 bands and half from water vapor bands (Figure 2).

4.3 | Nonlinear averaging

The multi-blackbody nonlinearity integrates to only $\Delta_M = -0.02$ W m^{-2} K^{-1} (green line in Figure 1b). Its largest contributions come from the O_3 ro-vibrational band and the flanks of the CO_2 ro-vibrational band, with negligible contributions at other wavenumbers, including water vapor bands (Figure 2). This ordering makes sense, because $\Delta_M^{\tilde{\nu}}$ depends on the width of the distribution of temperatures that are emitting to space at wavenumber $\tilde{\nu}$; this distribution is typically narrowest for water vapor, intermediate for CO_2, and widest for O_3. Water vapor concentrations drop rapidly with height, so emission to space in water vapor bands occurs from a narrow range of heights and temperatures at each wavenumber (e.g., Jeevanjee and Fueglistaler, 2020). Carbon dioxide is a well-mixed gas, so wavenumbers where CO_2 lines have $\tau_0 \approx 1$ will emit from a wider range of heights through the troposphere. Finally, O_3 is concentrated in the stratosphere and the underlying emission typically comes from close to the surface, so wavenumbers where O_3 lines have $\tau_0 \approx 1$ will emit from a bimodal distribution of heights and temperatures (with peaks at T_g and T_S), leading to greatest magnitudes of $\Delta_M^{\tilde{\nu}}$.

Spectral nonlinearity has a large magnitude at almost all wavenumbers, since most do not have $T_b^{\tilde{\nu}} \approx T_e$, and takes both positive and negative values, so for clarity it is not shown directly in Figure 1b. The cumulative integral of Δ_ν shows that positive contributions in the water vapor window region from 800-1200 cm^{-1}, where $T_b^{\tilde{\nu}} > T_e$, are only partly offset by negative contributions in strongly absorbing bands of CO_2, H_2O, and O_3, where $T_b^{\tilde{\nu}} < T_e$ (Figure 2). Notably, the negative contributions to Δ_ν by strongly absorbing bands are disproportionate to the greenhouse effect of each band, or the amount by which it reduces OLR. For example, the O_3 band and the H_2O rotation band each contribute about -0.05 W m^{-2} K^{-1} to Δ_ν, but the greenhouse effect of the water vapor rotational band is far larger. Similarly, the CO_2 ro-vibrational band and the H_2O ro-vibrational band each contribute about -0.2 W m^{-2} K^{-1} to Δ_ν, but the greenhouse effect of the CO_2 band is far larger. This mismatch arises because the high-wavenumber tail of the Planck function accounts for a disproportionately large share of $dB(T)/dT$ as compared to $B(T)$, so absorbers at high wavenumbers matter more in a relative sense for the Planck feedback than they do for OLR.

4.4 | Temperature-dependence of the corrections

Each correction term also depends on the surface temperature and absolute humidity of the reference-state atmosphere. By performing calculations with surface temperatures of 260-320 K, holding tropospheric relative humidity constant, I find that the Planck feedback varies more with surface temperature than does $4\sigma T_e^3$; λ_P can even exceed λ_e at high enough surface temperatures (Figure 3a). This greater sensitivity to temperature can be explained by the total local correction term $\Delta_S + \Delta_T + \Delta_M + \Delta_\nu$ becoming markedly less negative with surface warming and switching sign at $T_g = 320$ K (Figure 3). The temperature-dependence of the correction terms owes to the stratospheric masking and temperature-dependent opacity terms; nonlinear-averaging corrections vary little with surface temperature. As the surface warms at constant tropopause temperature, the stratosphere thins, stratospheric emissivity decreases, and Δ_S decreases in magnitude as well. The temperature-dependence of Δ_T occurs due to the competition between the water vapor continuum, which decreases in optical thickness with warming, and other absorption bands, which increase in optical thickness with warming. Water vapor continuum absorption becomes more important for $T_g > 300$K, shifting Δ_T from negative to positive values. These results indicate that the correction terms may lead to about a quarter of the meridional variation in the Planck feedback on Earth, with stratospheric masking and temperature-dependent opacity contributing roughly equally to the temperature-dependence of the Planck feedback. To my knowledge, this is a previously unrecognized aspect of the Planck feedback.

5 | DISCUSSION AND CONCLUSIONS

I have shown that the 0.5 W m^{-2} K^{-1} gap between the global Planck feedback, $\overline{\lambda_P}$, and the estimated feedback $\overline{\lambda_e} = 4\sigma\overline{T_e}^3$, can be closed with four correction terms. Meridional covariance is a result of global averaging and the covariance between polar-amplified warming and the weaker negative Planck feedback at the poles, and likely makes $\overline{\lambda_P}$ smaller than $\overline{\lambda_e}$ by around 0.25 W m^{-2} K^{-1}. Three other correction terms that affect the local Planck feedback – stratospheric masking, temperature-dependent opacity, and nonlinear averaging – have been defined and quantified for reference atmospheric profiles across a range of surface temperatures. For $T_g = 290$K, I find that stratospheric masking makes the largest contribution, reducing λ_P relative to λ_e by $\sim$ 0.35 W m^{-2} K^{-1} near global-mean surface temperatures. Temperature-dependent opacity also reduces λ_P by $\sim$ 0.1 W m^{-2} K^{-1}, but is compensated almost exactly by a $\sim$ 0.1 W m^{-2} K^{-1} increase in λ_P from nonlinear averaging, mainly from spectral nonlinearity. The stratospheric masking and temperature-dependent opacity corrections depend strongly on surface temperature, making λ_P more sensitive to local surface temperatures than λ_e would be, and likely contributing to the meridional gradient in the Planck feedback.

Stratospheric masking is consistently the largest negative correction to the local Planck feedback. Stratospheric masking can be included in a simple view of the total clear-sky longwave feedback – which includes Planck, water vapor, and lapse rate components – by slightly reframing the central result of Ingram (2010). Ingram (2010) clarified that to first order, spectral regions where water vapor makes the atmosphere optically thick show little increase in outgoing infrared flux with warming (at constant relative humidity), while all other wavenumbers will show a 'Planckian' increase in flux with warming (following $dB^{\tilde{\nu}}(T_b^{\tilde{\nu}})/dT$). Accounting for stratospheric masking revises this simple rule: any spectral regions that are not optically thick either to water vapor *or in the stratosphere* will to first-order show a 'Planckian' increase in flux with warming. Stratospheric optical thickness thus emerges as an important aspect of the clear-sky net longwave feedback that to my knowledge has not been previously considered.

I have assumed a relatively cold and isothermal stratosphere, which is likely to reduce the magnitude of Δ_S relative to calculations with a more realistic stratospheric temperature profile (Equation 15). Regarding the other corrections, use of a relatively cold stratosphere is unlikely to alter Δ_T much, as Δ_T depends only on the stratospheric emissivity and the tropopause flux increase with warming. A too-cold stratosphere might exaggerate the nonlinear-averaging corrections by increasing the variance of emitting temperatures. Therefore, calculations based on climate models with a more realistic stratospheric temperature profile might reveal an even more dominant role of the stratospheric masking correction.

Stratospheric temperatures should also respond to a change in upward flux at the tropopause if the stratosphere remains in radiative equilibrium, but this response is not included in standard calculations of the Planck feedback. The sensitivity of stratospheric temperatures and top-of-atmosphere fluxes to tropopause flux changes is likely nuanced, depending on both the spectral distribution of stratospheric emissivity and the base-state stratospheric temperature profile. The assumed lack of stratospheric temperature change embedded in standard Planck feedback calculations thus warrants further testing.

This work is intended to be illustrative rather than definitive, and I have used a line-by-line radiative transfer model to demonstrate how each correction arises as a consequence of specific greenhouse gases. Global climate models typically use radiation parameterizations that, for reasons of computational efficiency, solve radiative transfer equations at many fewer wavenumbers. For example, RRTMG (Clough et al., 2005) – a widely used scheme in climate models – uses the correlated-k approximation, in which the thermal spectrum is first broken up into broad bands (16 bands for RRTMG from 10-3250 cm^{-1}; a strong CO_2 band spans 630-700 cm^{-1}), and a small number of full radiative transfer calculations are then performed in each band by grouping wavenumbers with similar gas absorption coefficients. Thus, in RRTMG, only 140 radiative transfer calculations are done for each profile, and the temperature-dependence of absorption coefficients is represented by lookup tables rather than by explicit calculations of line strengths. Despite these differences, I have found with preliminary testing that all of the correction terms compare quite closely in magnitude between LBLRTM and RRTMG (not shown). Thus, I expect that the clear-sky Planck feedback calculated in climate models would have a similar breakdown of the correction terms to that presented here. I have quantified the meridional covariance correction only roughly; future work will include a more comprehensive assessment of this correction term by explicitly calculating Δ_C from climate model output (following equation 5).

This paper has focused on clear-sky conditions; cloud cover would modify the magnitudes of some correction terms. I expect stratospheric masking would remain the most important correction, and largely unaltered in magnitude, since stratospheric emissivity is independent of tropospheric clouds. By reducing the outgoing flux and smoothing its spectrum towards that of a blackbody at cloud-top temperature, optically thick cloud layers – especially in the upper troposphere – would likely reduce the magnitude of Δ_T and Δ_N. The behavior of the sum of the local correction terms, especially relative to the Planck feedback – which would also decrease greatly for a sky with thick high clouds – is less straightforward to anticipate. Low clouds are unlikely to greatly alter the picture presented in this paper. High and thin clouds might increase the magnitude of the multi-blackbody nonlinearity correction by increasing the variance of monochromatic brightness temperatures in many spectral regions. A greater variance of $T_b^{\tilde{\nu}}$ could also increase the magnitude of Δ_M under partly cloudy skies, but further quantifying this effect is deferred to future work.

Do these findings matter for climate sensitivity and the sum of climate feedbacks? In a narrow sense, the answer is no; I have merely explained aspects of the Planck feedback that, although poorly understood, are incorporated into climate model analysis and show relatively little inter-model spread. In a broader sense, however, this work clarifies how several properties of the climate system – stratospheric optical depth, temperature-dependence of absorption by greenhouse gases, and the location of spectral absorption features and window regions – may appreciably alter Earth's "no-feedback" climate sensitivity. Some of these properties may change slightly in the near future, and they could vary much more for distant past climates of Earth – or for climates of other worlds.

The stratospheric masking correction depends on stratospheric emissivity, which can be altered by anthropogenic greenhouse gases. Using the same reference temperature profile as in Figure 1, a doubling of CO_2 or of stratospheric water vapor (resulting from methane oxidation) both increase the magnitude of Δ_S by about 10% to -0.38 W m^{-2} K^{-1}, whereas a doubling of O_3 has a smaller impact, increasing the magnitude of Δ_S by only 0.01 W m^{-2} K^{-1} to -0.36 W m^{-2} K^{-1}. The historical combination of small decreases in global stratospheric Ozone, together with increases in carbon dioxide and stratospheric water vapor (e.g., Solomon et al., 2010), has likely made the Planck feedback less stabilizing due to increasing stratospheric opacity. Although these effects are minor in the historical period, they will grow in the future and should be accounted for in feedback analysis of climate model simulations that use CO_2 concentrations many times larger than present values.

As an example of how a much larger change in atmospheric composition could alter the Planck feedback, I have done a calculation where CO_2 (400 ppmv) is removed from the reference case (Figure 1) and replaced with 2.3% CH_4 by volume – an amount tuned to give the same $F_0 = 249.4$ W m^{-2} (Figure 4). As noted in Pierrehumbert (2010), much more methane is required than carbon dioxide to give the same greenhouse effect if only one of the two gases is present, because methane's ro-vibrational band around 1250 cm^{-1}, unlike carbon dioxide's ro-vibrational band near 666 cm^{-1}, is offset considerably in wavenumber from the peak in the Planck function for Earth's atmospheric temperatures. By construction, this example has the same value of $\lambda_e = 3.87$ W m^{-2} K^{-1} as the reference case, but it has $\lambda_P = 3.32$ W m^{-2} K^{-1}, 0.2 W m^{-2} K^{-1} lower than the reference case, and a notably different composition of the correction terms. Spectral nonlinearity has switched signs and is now the largest negative correction term at -0.26 W m^{-2} K^{-1}, stratospheric masking has decreased in magnitude to -0.25 W m^{-2} K^{-1}, multi-blackbody nonlinearity has remained about the same, and temperature-dependent opacity has decreased in magnitude to only -0.02 W m^{-2} K^{-1}. The large negative contribution of spectral nonlinearity occurs because the absorption lines of CH_4 lie almost entirely above 1000 cm^{-1}; methane thus contributes far more in a relative sense to reducing dF_0/dT_T than to reducing F_0. This example highlights that greenhouse gases with absorption features at high wavenumbers could be more important for climate feedbacks than their impact on outgoing radiation would suggest.

I have also done an example calculation under conditions reminiscent of snowball Earth, with 10% CO_2 by volume, $T_g = 260$ K, and a lower $T_S = 190$ K (Figure 5). The total correction to the Planck feedback in this case is -0.73 W m^{-2} K^{-1}, dominated by stratospheric masking (-0.54 W m^{-2} K^{-1}) and temperature-dependent opacity (-0.22 W m^{-2} K^{-1}). The correction terms combine to reduce λ_P by over 25 % relative to λ_e, and the sum of Planck, water vapor, and lapse rate feedbacks for this atmosphere would be only 1.3 W m^{-2} K^{-1} (calculated by comparing to the OLR from a calculation with $T_g = 261$ K). In this situation, the corrections to the Planck feedback are as large as the combined water vapor and lapse rate feedback, and the climate would be quite sensitive to radiative forcing even without including cloud or surface albedo feedbacks.

This paper has explored a subject that most climate scientists would likely consider so simple as to be trivial, and found hidden subtleties in the Planck feedback. These subtleties should be considered explicitly at the level of detail for which feedback analysis is conducted in climate models. In addition to providing a novel exposition of several corrections to the Planck feedback, which could be viewed as important feedback mechanisms in their own right, this work also serves as a reminder: in the climate system, few things are as simple as they may seem.

APPENDIX A: DEPENDENCE OF LINE STRENGTH ON TEMPERATURE

Quantitatively, if the intensity of an absorption line S centered at wavenumber $\tilde{\nu}_c$ is known at temperature T_0, then the line intensity at some other temperature T is given by:

$$S(T) = S(T_0)\frac{Q(T_0)}{Q(T)}\left[\frac{1-e^{-\frac{hc\tilde{\nu}_c}{kT}}}{1-e^{-\frac{hc\tilde{\nu}_c}{kT_0}}}\right]e^{-\frac{hc\tilde{\nu}_l}{k}\left(\frac{1}{T}-\frac{1}{T_0}\right)}, \tag{23}$$

where $hc\tilde{\nu}_l$ is the energy of the lower-level state for the transition, and $Q(T)$ and $Q(T_0)$ are the total internal partition function at temperatures T and T_0, respectively (Rothman et al., 1998). The dominant temperature-dependence for most lines arises from the final term $e^{-\frac{hc\tilde{\nu}_l}{k}\left(\frac{1}{T}-\frac{1}{T_0}\right)}$, or ratio of Boltzmann factors for the lower-level state at temperature T relative to temperature T_0; temperature-dependence of $Q(T)$ and of the bracketed term are comparatively weak unless the lower-level energy is small relative to the thermal energy (e.g., $hc\tilde{\nu}_l < kT$). This can be shown by looking at the relative change in line intensity with warming:

$$\frac{d\log S}{dT} = -\frac{d\log Q}{dT} - \frac{hc\tilde{\nu}_c}{kT^2}\frac{e^{-\frac{hc\tilde{\nu}_c}{kT}}}{1-e^{-\frac{hc\tilde{\nu}_c}{kT}}} + \frac{hc\tilde{\nu}_l}{kT^2}. \tag{24}$$

As an example, consider CO_2 at 260 K, and a relatively strong line somewhat away from the center of the ro-vibrational feature, near 600 cm^{-1}, with $\tilde{\nu}_l \sim 1000$ cm^{-1}. In this situation, $Q \sim T$ (Pierrehumbert, 2010), so the partition function term contributes a $\sim -0.4\%$ K^{-1} line weakening, the second term contributes negligibly, and the Boltzmann factor term contributes about a $\sim 2.1\%$ K^{-1} line strengthening. Such an increase in opacity, depending on how optically thick the atmosphere is near the line center, can lead to a marked compensation for the increased Planck function source with warming.

APPENDIX B: SIGN AND MAGNITUDE OF THE MULTI-BLACKBODY NONLINEARITY

For a collection of blackbodies, the increase in flux with uniform warming is proportional to the average of the cubes of their temperatures, whereas the estimate $4\sigma T_e^3$ is related to the 3/4 power of the average of the fourth powers of their temperatures. Specifically, letting w_i represent the weighting of temperature T_i in a collection of n blackbodies (where the w_i sum to unity), the increase in flux with uniform warming is $4\sigma\left[\sum_{i=1}^{n} w_i T_i^3\right]$, whereas the estimated increase is $4\sigma\left[\sum_{i=1}^{n} w_i T_i^4\right]^{3/4}$. Raising both expressions to the 1/3 power reveals that they are power means of the temperatures in the collection of blackbodies, with the cube root of the flux increase given by $(4\sigma)^{1/3}\left[\sum_{i=1}^{n} w_i T_i^3\right]^{1/3}$ (a power mean of degree 3), and the cube root of $4\sigma T_e^3$ given by $(4\sigma)^{1/3}\left[\sum_{i=1}^{n} w_i T_i^4\right]^{1/4}$ (a power mean of degree 4). The generalized mean inequality (e.g., Hardy et al., 1952, theorem 19) proves that a mean of higher degree is greater than or equal to a mean of lower degree; thus $4\sigma T_e^3$ must be greater than or equal to the actual flux increase.

As a more concrete example, consider a collection of blackbodies with temperature distributed uniformly in $[\overline{T} - \delta T/2, \overline{T} + \delta T/2]$. Letting $u = \delta T/\overline{T}$ and using x as an integration variable over the distribution (so that $T(x) = \overline{T} + x\delta T = \overline{T}(1 + ux)$), the mean OLR from this collection of blackbodies is given by:

$$\mathrm{OLR} = \sigma\overline{T}^4 \int_{-1/2}^{1/2} \left(1 + 4ux + 6u^2x^2 + 4u^3x^3 + u^4x^4\right) dx = \sigma\overline{T}^4 \left(1 + \frac{u^2}{2} + \frac{u^4}{80}\right). \tag{25}$$

Since $T_e = (\mathrm{OLR}/\sigma)^{1/4}$, it follows that:

$$4\sigma T_e^3 = 4\sigma\overline{T}^3 (1 + u^2/2 + u^4/80)^{3/4}. \tag{26}$$

The flux increase for a uniform warming of the whole distribution of blackbodies is given by:

$$\int_{-1/2}^{1/2} 4\sigma T^3(x) dx = 4\sigma\overline{T}^3 (1 + u^2/4), \tag{27}$$

so the correction Δ_M due to multiple-blackbody nonlinearity in this simple situation would be:

$$\begin{aligned}
\Delta_M &= \int_{-1/2}^{1/2} 4\sigma T^3(x) dx - 4\sigma T_e^3 \\
&= 4\sigma\overline{T}^3 \left[(1 + u^2/4) - (1 + u^2/2 + u^4/80)^{3/4}\right] && (28) \\
&\approx -4\sigma\overline{T}^3 (u^2/8), && (29)
\end{aligned}$$

where the binomial approximation on the last line has assumed $u << 1$. If the distribution of blackbodies here were taken to represent different emission levels in the vertical, with emitting temperatures between roughly 200 K and 300K in Earth's Tropics, then $u \approx 0.4$ and the magnitude of Δ_M would be about 2% of λ_P, or about –0.07 W m^{-2} K^{-1}. If the distribution of blackbodies instead represented different emission temperatures across latitude bands, temperatures might range from 230 K to 270 K, so $u \approx 0.16$ and the correction from the multiple-blackbody nonlinearity would be much smaller, only 0.3% or –0.01 W m^{-2} K^{-1}. Thus, multi-blackbody nonlinearity could be a significant factor in reducing the local Planck feedback, but likely has little effect on averaging across latitudes relative to the aforementioned meridional covariance correction. Furthermore, since the distribution of temperatures that emit to space at a given wavenumber is usually much narrower than the distribution of brightness temperatures across the spectrum, monochromatic calculations of Δ_M (equation 18) will typically make this correction factor even smaller in magnitude.

ACKNOWLEDGEMENTS

Work on this paper was supported by NSF Atmospheric Chemistry grant AGS-1906719: "Advancing the Understanding of the Impacts of Wave-Induced Temperature Fluctuations on Atmospheric Chemistry". I thank Susan Solomon, Peter Molnar, Nick Lutsko, Daniel Koll, and Aaron Donohoe for helpful comments on drafts of this manuscript, and AER for freely providing LBLRTM (available at `http://rtweb.aer.com/lblrtm.html`). Model output and scripts used to make figures in this paper are available at `https://www.dropbox.com/sh/9vrn1v4brxj2m7m/AACp1jELMc1OfLWo3ZoBDwsma?dl=0`.

REFERENCES

Cess, R. D., Potter, G. L., Blanchet, J. P., Boer, G. J., Genio, A. D. D., Deque, M., Dymnikov, V., Galin, V., Gates, W. L., Gahn, S. J., Kiehl, J. T., Lacis, A. A., Treut, H. L., Li, Z.-X., Liang, X.-Z., McAvaney, B. J., Meleshko, V. P., Mitchell, J. F. B., Morcrette, J.-J., Randall, D. A., Rikus, L., Roeckner, E., Royer, J. F., Schlese, U., Sheinin, D. A., Slingo, A., Sokolov, A. P., Taylor, K. E., Washington, W. M., Wetherald, R. T., Yagai, I. and Zhang, M.-H. (1990) Intercomparison and interpretation of climate feedback processes in 19 atmospheric general circulation models. *Journal of Geophysical Research*, **95**, 16601–16615.

Clough, S. A., Shephard, M. W., Mlawer, E. J., Delamere, J. S., Iacono, M. J., Cady-Pereira, K., Boukabara, S. and Brown, P. D. (2005) Atmospheric radiative transfer modeling: A summary of the AER codes. *J. Quant. Spectrosc. Radiat. Transfer*, **91**, 233–244.

Cormier, J. G., Hodges, J. T. and Drummond, J. R. (2005) Infrared water vapor continuum absorption at atmospheric temperatures. *The Journal of Chemical Physics*, **122**.

Feldl, N. and Roe, G. H. (2013) Four perspectives on climate feedbacks. *Geophysical Research Letters*, **40**, 4007–4011.

Hardy, G. H., Littlewood, J. E. and Polya, G. (1952) *Inequalities.* Cambridge University Press.

Ingram, W. (2010) A very simple model for the water vapour feedback on climate change. *Quarterly Journal of the Royal Meteorological Society*, **136**, 30–40.

Jeevanjee, N. and Fueglistaler, S. (2020) On the cooling to space approximation. *Journal of the Atmospheric Sciences*, **77**, 465–478.

Merlis, T. and Henry, M. (2018) Simple estimates of polar amplification in moist diffusive energy balance models. *Journal of Climate*, **31**, 5811–5824.

North, G. R. and Coakley, J. A. (1979) Differences between seasonal and mean annual energy balance model calculations of climate and climate sensitivity. *The Journal of the Atmospheric Sciences*, **36**, 1189–1204.

Pierrehumbert, R. (2010) *Principles of Planetary Climate*. Cambridge, UK: Cambridge University Press.

Rothman, L. S., Rinsauld, C. P., Goldman, A., Massie, S. T., Edwards, D. P., Flaud, J.-M., Perrin, A., Camy-Peyret, C., Dana, V., Mandin, J.-Y., Schroeder, J., McCann, A., Gamache, R. R., Wattson, R. B., Yoshino, K., Chance, K. V., Jucks, K. W., Brown, L. R., Nemtchinov, V. and Varanasi, P. (1998) The HITRAN molecular spectroscopic database and HAWKS (HITRAN atmospheric workstation): 1996 edition. *Journal of Quantitative Spectroscopy and Radiative Transfer*, **60**, 665–710.

Shine, K. P., Ptashnik, I. V. and Radel, G. (2012) The water vapor continuum: brief history and recent developments. *Surveys in Geophysics*, **33**, 535–555.

Soden, B. J. and Held, I. M. (2006) An assessment of climate feedbacks in coupled ocean-atmosphere models. *Journal of Climate*, **19**, 3354–3360.

Soden, B. J., Held, I. M., Colman, R., Shell, K. M., Kiehl, J. T. and Shields, C. A. (2008) Quantifying climate feedbacks using radiative kernels. *Journal of Climate*, **21**, 3504–3520.

Solomon, S., Rosenlof, K. H., Portmann, R. W., Daniel, J. S., Davis, S. M., Sanford, T. J. and Plattner, G.-K. (2010) Contributions of stratospheric water vapor to decadal changes in the rate of global warming. *Science*, **327**, 1219–1223.

Wing, A. A., Reed, K. A., Satoh, M., Stevens, B., Bony, S. and Ohno, T. (2018) Radiative-convective equilibrium model intercomparison project. *Geoscientific Model Development*, **11**, 793–813.

Zelinka, M. D., Meyers, T. A., McCoy, D. T., Po-Chedley, S., Caldwell, P. M., Ceppi, P., Klein, S. A. and Taylor, K. E. (2020) Causes of higher climate sensitivity in CMIP6 models. *Geophysical Research Letters*, **47**.

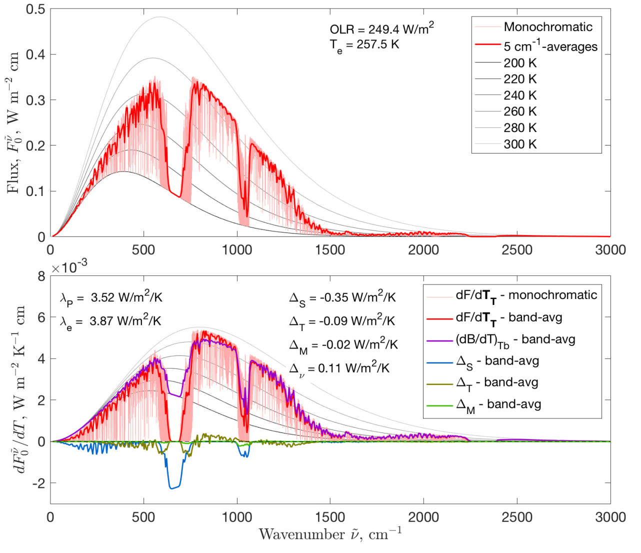

FIGURE 1 a) Outgoing infrared flux spectrum with the line-by-line radiative transfer model LBLRTM, for an atmosphere with a surface temperature of 290 K. The pink curve indicates monochromatic irradiances, and the red curve irradiances averaged over 5 cm^{-1} wavenumber bands. Thin lines from black to light gray show reference blackbody spectra. b) Changes in OLR flux spectrum for: 1K of troposphere and surface warming (monochromatic change in pink, average over 5 cm^{-1} bands in red), for 1K increase in monochromatic brightness temperature (purple), and for the correction terms $\Delta_S^{\tilde{\nu}}$, $\Delta_T^{\tilde{\nu}}$, and $\Delta_M^{\tilde{\nu}}$ (blue, gold, and green, respectively). Thin lines from black to light gray show the derivative of the Planck function for the same reference temperatures as in a).

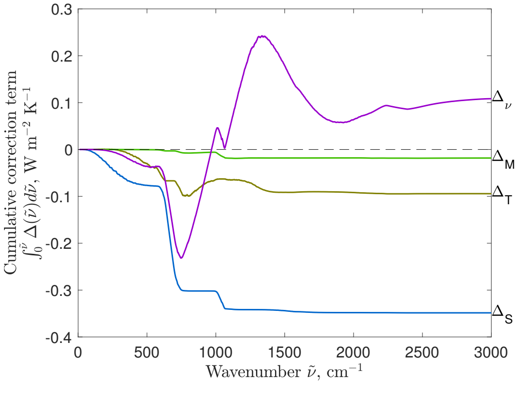

FIGURE 2 Cumulative integrals from 0 to wavenumber $\tilde{\nu}$ of each correction term to the local Planck feedback. The value at the right-hand side of the plot indicates the full value of the correction term Δ, and wavenumbers of greatest slope indicate areas most important to the value of the correction term.

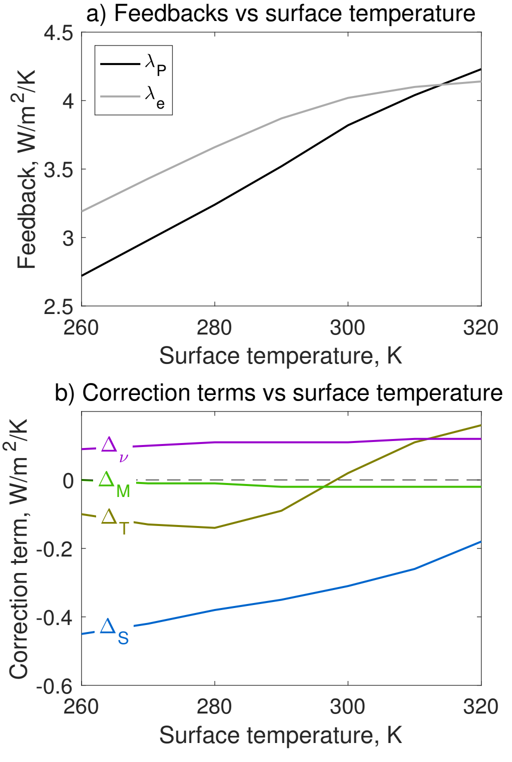

FIGURE 3 a) Planck feedback λ_P and estimated feedback $\lambda_e = 4\sigma T_e^3$ over a range of surface temperatures. b) Spectrally integrated correction terms for stratospheric masking (Δ_S), temperature-dependent opacity (Δ_T), and nonlinear averaging (Δ_M and Δ_ν) over a range of surface temperatures.

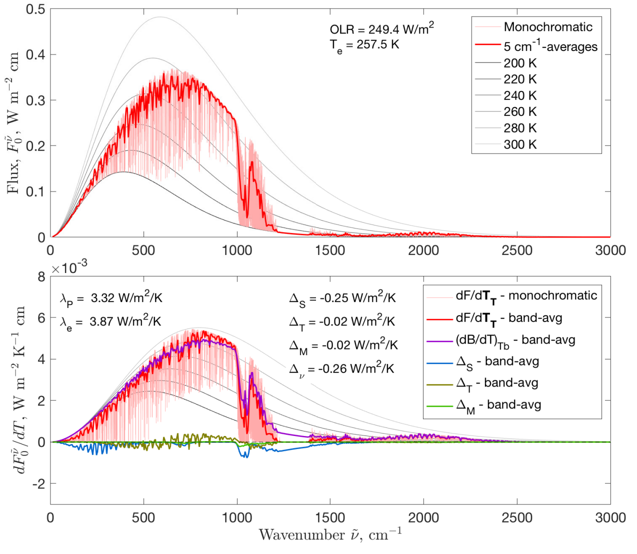

FIGURE 4 As in Figure 1 but for an atmosphere with no CO_2 and instead 2.3 % CH_4. a) Outgoing infrared flux spectrum; b) Changes in OLR flux spectrum for different cases and spectra of different correction terms.

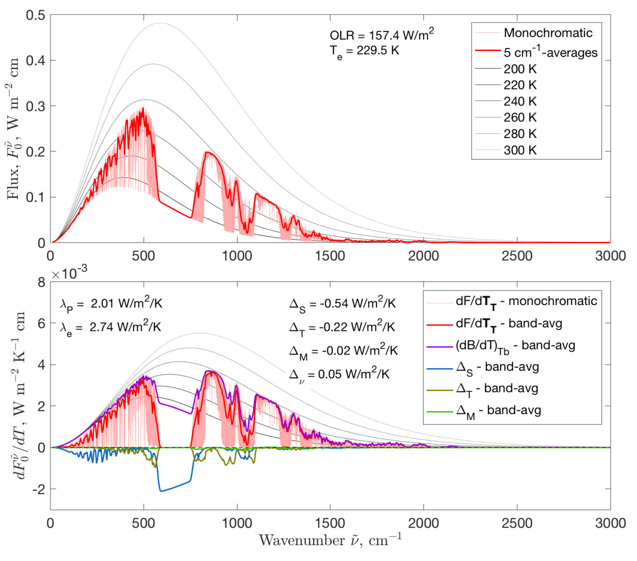

FIGURE 5 As in Figure 1 but for a snowball-like scenario with 10% CO_2, a surface temperature of 260 K, and a stratospheric temperature of 190 K. a) Outgoing infrared flux spectrum; b) Changes in OLR flux spectrum for different cases and spectra of different correction terms.